

Magnetic properties of RFeSi (R≡La–Sm, Gd–Dy) from susceptibility measurements and neutron diffraction studies

R. Welter, G. Venturini and B. Malaman

Laboratoire de Chimie du Solide Minéral, associé au CNRS 158, Université de Nancy I, BP 239, 54506, Vandoeuvre les Nancy Cedex (France)

(Received April 6, 1992)

Abstract

Investigations made by susceptibility measurements and neutron diffraction experiments are reported on the ternary silicides RFeSi (R≡La–Sm, Gd–Dy) with the tetragonal CeFeSi-type structure (space group, $P4/nmm$). This structure, which is closely related to the ThCr_2Si_2 - and TbFeSi_2 -type structures, can be described as isolated ThCr_2Si_2 blocks connected via R–R contacts. LaFeSi and CeFeSi are Pauli paramagnets, whereas PrFeSi is a Curie–Weiss paramagnet down to 2 K. The other compounds are ferromagnetic below $T_C=25, 40, 135, 125$ and 110 K for neodymium, samarium, gadolinium, terbium and dysprosium respectively. With the exception of GdFeSi, these compounds exhibit rather large coercive fields at 4.2 K (up to 9 kOe for terbium). Neutron diffraction experiments on RFeSi (R≡Nd, Tb, Dy) led to the determination of collinear ferromagnetic structures with magnetic moments (with values close to the theoretical free ion values) localized on R ions only and aligned along the c axis. The results are discussed and compared with those of closely related RFe_2Si_2 and RFeSi₂ compounds.

1. Introduction

The magnetic properties of ternary rare earth transition metal silicides and germanides have been extensively studied over the last 10 years. The most important work has been devoted to the ThCr_2Si_2 representatives [1]. More recently, we reported the magnetic properties of RMnSi_2 and RFeSi_2 compounds [2–4] which crystallize in the closely related TbFeSi_2 -type structure [5]. In order to complete the systematic study of these phases, we have investigated the equiatomic RFeSi and RMnSi series. These compounds have been known for more than 12 years [6, 7], but for the iron compounds, with the exception of CeFeSi and GdFeSi, no elaborate study of their physical properties has been made [8–10]. In this paper, we report the magnetic properties of the iron compounds.

The silicides RFeSi (R≡La–Sm, Gd–Ho) were first synthesized by Bodak *et al.* [6]. They crystallize in the tetragonal structure of CeFeSi (space group, $P4/nmm$) in which the R(cerium), iron and silicon atoms occupy the 2(c) [$\frac{1}{2}, \frac{1}{2}, z_R \approx 0.67$], 2(a) [$\frac{1}{2}, \frac{1}{2}, 0$] and 2(c) [$\frac{1}{2}, \frac{1}{2}, z_{\text{Si}} \approx 0.17$] site respectively. This structure is built of alternating (001) square planes containing R, iron and silicon atoms respectively. The corresponding sequence can be represented by $\text{RSiFe}_2\text{SiR}-\text{RSiFe}_2\text{SiR}$. The tran-

sition metal plane is twice as dense as the silicon and R planes. This structure is closely related to the ThCr_2Si_2 - and TbFeSi_2 -type structures in which the same atoms lie in alternate layers along the c and b axes with the sequences $\text{RSiT}_2\text{SiRSiT}_2\text{Si}$ and $\text{RSiT}_2\text{SiRSi}-\text{SiRSiT}_2\text{SiR}$ respectively (Fig. 1). Therefore the same [R–Si–T₂–Si–R] block is found in each type of structure with additional R–R and R–Si–Si–R sequences in CeFeSi and TbFeSi_2 respectively. In all cases, the silicon atoms form tetrahedra around the transition metal atoms T with very short T–Si distances suggesting covalent bonding. The R and T atoms form square lattices with R–R and T–T distances close to 4 Å and 2.9 Å respectively (Fig. 1). These three structural types can therefore be regarded as stacking variants of metal atom planes, the stacking being more or less anisotropic. Figure 1 clearly shows the structural relationships.

The magnetic properties of RFe_2Si_2 and RFeSi_2 have been described. Earlier reports on the RFe_2Si_2 series (see ref. 1 where a large review on the magnetic properties of these compounds can be found) and RFeSi_2 [2, 4] claim that iron atoms have no magnetic moment and only the R atoms eventually show magnetic long-range ordering at low temperature. PrFe_2Si_2 [11] and NdFe_2Si_2 [12] were found to order antiferromagnetically

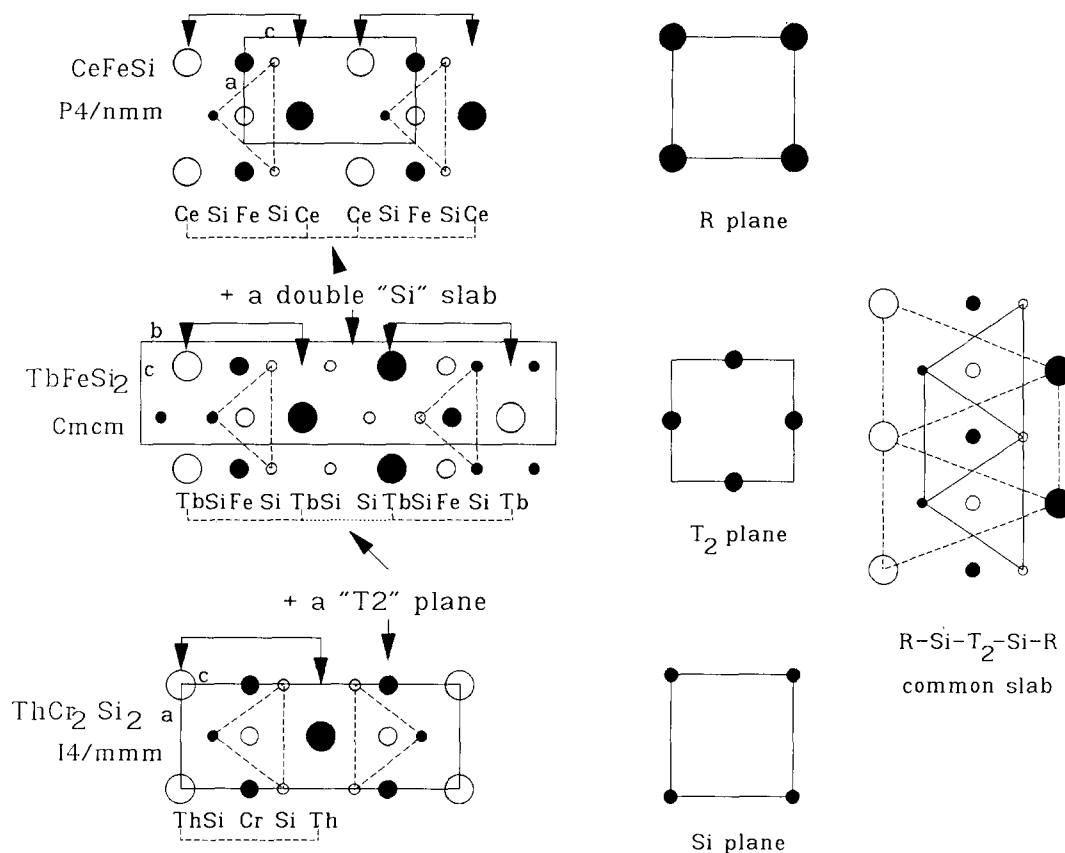


Fig. 1. Structural relationships between $CeFeSi$ -, $TbFeSi_2$ - and $ThCr_2Si_2$ -type structures. R , T_2 and Si planes and common $[RSiFe_2SiR]$ " $ThCr_2Si_2$ -type" block are shown.

with the AFII type (see Fig. 23 of ref. 1) below 8 and 15.6 K respectively. The compounds with gadolinium, terbium, dysprosium and holmium exhibit incommensurate antiferromagnetic behaviour of the LSWIV type (see Fig. 23 of ref. 1). On the other hand, $PrFeSi_2$ orders ferromagnetically at 26 K, whereas $NdFeSi_2$ exhibits a modulated antiferromagnetic structure below 6.5 K [4]. In all cases, the structure corresponds to a stacking of ferromagnetic R sheets with the moments perpendicular to the sheets.

As we have indicated, the $CeFeSi$ -type structure can be considered, in terms of anisotropy and interactions between magnetic atoms, as an intermediate situation between the RFe_2Si_2 - and $RFeSi_2$ -type structures. Hence, it is of interest to study their magnetic properties in order to specify the magnetic interactions in this class of materials with highly anisotropic structures.

In this study, we investigate the magnetic properties of the $RFeSi$ ($R \equiv La-Sm, Gd-Dy$) compounds using bulk magnetization measurements and examine the magnetic structures of the $NdFeSi$, $DyFeSi$ and $TbFeSi$ compounds using neutron diffraction experiments. A comparison with the RFe_2Si_2 and $RFeSi_2$ compounds and a general discussion are given in the conclusion.

2. Experimental procedures

The compounds were prepared from commercially available high-purity elements. Pellets of stoichiometric mixture were compacted using a steel die and then introduced into silica tubes sealed under argon (100 mmHg). The samples were heated at 1173 K for preliminary homogenization treatment and then melted in an induction furnace. The resulting ingots were annealed for 2 weeks at 1173 K. The purity of the final product was checked by the X-ray powder diffraction technique (Guinier $Cu K\alpha$ and curved detector INEL CPS 120 $Co K\alpha$).

The magnetic measurements were carried out on a Faraday balance (above 300 K) and on a FONER magnetometer (between 4.2 and 300 K), in fields up to 2 T.

Neutron diffraction experiments were carried out at the Institut Laue Langevin (ILL), Grenoble. The diffraction patterns were recorded with the one-dimension curved multidetector D1b at a wavelength $\lambda = 2.5293$ Å. In the case of $DyFeSi$, a special double-walled vanadium sample holder was used in order to minimize neutron absorption. Several patterns were collected in

the temperature range 2–150 K, namely above and below the ordering temperature for each compound. The first refinements, carried out with the neutron pattern recorded in the paramagnetic state, pointed to the occurrence of texture effects (due to tablet-like crystallites; the c axis takes a preferential orientation perpendicular to the neutron beam). In order to correct this effect we followed the suggestion of Dollase [13] and used the March formula [14]

$$M_{hkl} = \left(f_{\text{cor}} \cos^2 \alpha + \frac{\sin^2 \alpha}{f_{\text{cor}}} \right)^{-3/2}$$

where M_{hkl} is a corrective factor for the calculated intensity of each line, f_{cor} is a fitted coefficient which reflects the importance of preferential orientation and α is the angle between the c axis and the hkl plane in the Bragg position. The value of f_{cor} obtained for refinements of each compound (see below) strongly supports the validity of this correction. Using the Fermi lengths tabulated by Freeman and Declaux [15] and the magnetic form factor of Nd^{3+} , Dy^{3+} and Tb^{3+} ions taken from ref. 16, the scaling factor f_{cor} , the atomic positions z_{R} and z_{Si} and the R magnetic moments were refined by the MXD least-squares fitting procedure [17]. The MXD program allows the simultaneous fitting of the nuclear and magnetic intensities with those observed.

3. Experimental results

Our syntheses confirm that the RFeSi series extends from LaFeSi to HoFeSi. Lattice parameters refined at room temperature (Table 1) are in quite good agreement with the earlier values of Bodak *et al.* [6]. Their evolution with the radius of the rare earth atoms suggests that cerium is in a mixed valent state in CeFeSi. Only HoFeSi could not be prepared sufficiently pure for the magnetic study.

3.1. Susceptibility measurements

The main characteristic magnetic data are collected in Table 2.

3.1.1. Paramagnetic state

LaFeSi exhibits weak Pauli paramagnetic behaviour indicating that iron does not carry any moment as also observed in RFe_2Si_2 and RFeSi_2 compounds [1, 2]. In CeFeSi, cerium appears to be in an intermediate valent state in agreement with the conclusions derived from the lattice parameter variations observed in this series (Table 1). A similar behaviour has been observed in CeFe_2Si_2 and CeFeSi_2 [1, 2]. The other silicides (R≡Pr–Sm, Gd–Tb) are paramagnetic at room temperature and the temperature dependence of their inverse magnetic susceptibilities obeys a Curie–Weiss-type law, except for SmFeSi. The experimental effective moment values are in good accordance with the theoretical R^{3+} free ion values (Table 2); the lack of moment on iron in these compounds is thus confirmed.

3.1.2. Magnetic state

No magnetic transition is observed above 4.2 K for PrFeSi, whereas the other silicides RFeSi (R≡Nd, Sm, Gd–Tb) are characterized by ferromagnetic transitions (due to the ordering of the rare earth sublattices) at high temperatures ($T_{\text{C}}=25, 40, 135, 125$ and 110 K for NdFeSi, SmFeSi, GdFeSi, TbFeSi and DyFeSi respectively). With the exception of GdFeSi, the aspect of the thermomagnetic curves is characteristic of the existence of a strong magnetic anisotropy (Fig. 2(a)). This observation is in agreement with the moment values measured at 4.2 K in 20 kG, which are substantially lower than the theoretical values of the free ion moments. Moreover, some of these compounds display ample coercive fields (TbFeSi ≈ 9 kG at 4.2 K), which points to a strong uniaxial anisotropy in this class of materials (Fig. 2(b), Table 2).

TABLE 1. RFeSi: lattice parameters at room temperature

Compound	This work			Bodak <i>et al.</i> [6]		
	a (Å)	c (Å)	V (Å ³)	a (Å)	c (Å)	V (Å ³)
LaFeSi	4.096(4)	7.133(7)	119.7	4.062(3)	7.179(5)	118.5
CeFeSi	4.086(2)	6.788(3)	113.3	4.062(3)	6.927(5)	114.9
PrFeSi	4.076(2)	6.952(4)	115.5	4.057(3)	6.893(5)	113.5
NdFeSi	4.069(1)	6.918(2)	114.5	4.031(3)	6.828(5)	110.8
SmFeSi	4.035(2)	6.831(3)	111.2	4.001(3)	6.793(5)	108.8
GdFeSi	4.001(3)	6.818(4)	109.2	3.984(3)	6.751(5)	107.2
TbFeSi	3.975(2)	6.778(3)	107.1	3.961(3)	6.745(5)	105.8
DyFeSi	3.948(2)	6.844(4)	106.7	3.937(3)	6.774(5)	105.0

TABLE 2. RFeSi: magnetic data

Compound	T_C (± 2) (K)	Θ_P (K)	μ_{eff} (μ_B)	$g\{J(J+1)\}^{1/2}$ (μ_B)	H_C (4.2 K) (kG)	M (4.2 K, 20 kG) (μ_B)	gJ (μ_B)
LaFeSi	—	—	—	0	—	—	0
CeFeSi	—	—	—	2.54	—	—	2.14
PrFeSi	—	35	3.62	3.58	—	—	3.2
NdFeSi	25	20	3.90	3.62	1.4	1.4	3.28
SmFeSi ^a	40	—	—	0.84	2.2	0.3	0.72
GdFeSi	135	165	8.09	7.94	0.0	7.1	7
TbFeSi	125	110	9.62	9.72	9	4.1	9
DyFeSi	110	75	10.57	10.63	5.4	5.2	10

^aSmFeSi susceptibility does not follow a Curie-Weiss behaviour.

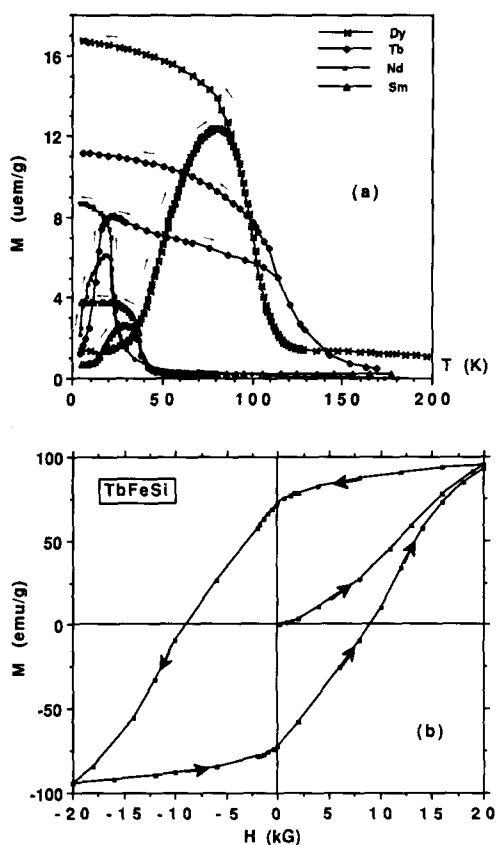


Fig. 2. (a) Temperature dependence of the magnetization ($H_{\text{app}} = 500$ Oe) in RFeSi (R=Nd, Sm, Tb, Dy) compounds. (b) Hysteresis loop at 4.2 K in TbFeSi.

In GdFeSi ($H_C = 0$), the saturation moment value corresponds to the calculated value (gJ) in the ordered state (Table 2). This result is in agreement with the isotropic behaviour of the Gd^{3+} ion.

In order to specify the magnetic behaviour of these compounds, we have undertaken neutron diffraction experiments. SmFeSi and GdFeSi have not been studied as the samarium and gadolinium absorption coefficients are too large at the wavelength used (2.5293 Å).

3.2. Neutron diffraction study

3.2.1. Crystal structure

The neutron diffraction patterns recorded in the paramagnetic state are characteristic of only the nuclear scattering (Fig. 3). The extinction rules of the space group $P4/nmm$ are fulfilled and confirm unambiguously the CeFeSi-type structure for NdFeSi, TbFeSi and DyFeSi. Attempts to fit the nuclear lines by interchanging the positions of the iron and silicon atoms lead to a poorer agreement and give no evidence for any mixing between the iron and silicon atoms in 2(a) and 2(c) sites. A comparison between the observed and calculated intensities of the nuclear peaks for each compound is given in Tables 3–5, together with the z_R and z_{Si} values, f_{cor} , the reliability factors and the lattice parameters.

3.2.2. Magnetic structures

At 2 K, the data obtained show only an increase in the intensity of the nuclear reflection (except for (001) and (003) peaks), indicating the occurrence of ferromagnetic ordering. The absence of magnetic contributions to the (00 l) reflections shows that the moments are aligned along the c axis. The magnetic structure is shown in Fig. 4. It corresponds to a stacking of (001)

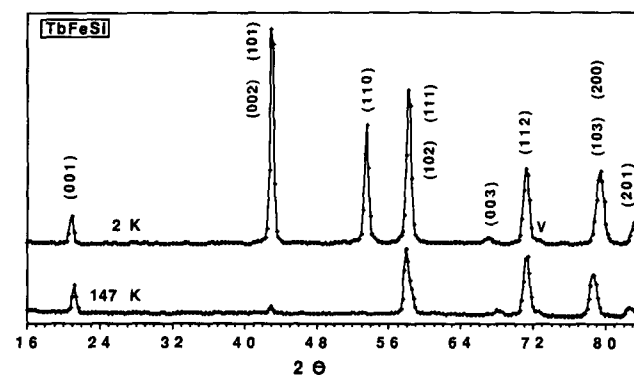


Fig. 3. Neutron diffraction patterns of TbFeSi at 147 and 2 K.

TABLE 3. NdFeSi: observed and calculated intensities and refined parameters

<i>hkl</i>	138 K		2 K	
	I_o	I_c	I_o	I_c
001	7.2(1)	7.1	7.3(1)	6.6
101	9.0(1)	8.7	30.6(2)	30.0
002	0.6(1)	0.5	1.8(3)	0.6
110	4.0(2)	3.1	25.9(4)	27.1
111	111.3(4)	113.0	120.7(1)	122.9
102	54.1(3)	53.5	62.0(2)	61.1
003	20.1(3)	19.2	21.2(1)	18.5
112	198.4(8)	198.2	195.0(8)	195.9
103 } 200 } 201 }	242.1(7)	241.1	269.3(1)	267.8
	56.5(5)	59.0	61.4(2)	65.4
	$R=0.010$	$f_{\text{cor}}=1.23(1)$	$R=0.016$	$f_{\text{cor}}=1.25(1)$
	$z_{\text{Si}}=0.179(2)$	$z_{\text{Nd}}=0.677(1)$	$z_{\text{Si}}=0.179(3)$	$z_{\text{Nd}}=0.675(1)$
				$\mu_{\text{Nd}}=2.58(8) \mu_{\text{B}}$
	$a=4.069(2) \text{ \AA}$	$c=6.902(3) \text{ \AA}$	$a=4.070(2) \text{ \AA}$	$c=6.887(3) \text{ \AA}$

TABLE 4. TbFeSi: observed and calculated intensities and refined parameters

<i>hkl</i>	147 K		2 K	
	I_o	I_c	I_o	I_c
001	7.1(1)	7.1	7.8(1)	7.6
101 } 002 } 110 }	6.4(2)	5.8	233.1(8)	234.1
	2.0(4)	1.9	207.8(18)	209.7
111 } 102 } 003 }	130.5(6)	123.6	336.7(13)	335.2
	45.4(6)	45.4	16.2(12)	24.5
	16.9(5)	26.7	275.0(14)	273.0
112 } 103 } 200 } 201 }	218.0(1)	217.3	368.3(22)	367.0
	206.6(2)	210.8	—	—
	47.4(9)	44.4		
	$R=0.039$	$f_{\text{cor}}=1.14(3)$	$R=0.014$	$f_{\text{cor}}=1.15(2)$
	$z_{\text{Si}}=0.209(9)$	$z_{\text{Tb}}=0.672(4)$	$z_{\text{Si}}=0.202(9)$	$z_{\text{Tb}}=0.676(1)$
				$\mu_{\text{Tb}}=8.82(7) \mu_{\text{B}}$
	$a=3.971(2) \text{ \AA}$	$c=6.741(3) \text{ \AA}$	$a=3.943(2) \text{ \AA}$	$c=6.833(3) \text{ \AA}$

ferromagnetic sheets, with moments perpendicular to the sheets.

A different behaviour is observed for PrFeSi. In this compound, at 2 K, no magnetic contribution is found in the diffraction pattern, in agreement with the bulk magnetization results.

The values of the magnetic moments on the neodymium, terbium and dysprosium atoms are 2.58(8), 8.82(7) and 9.81(16) μ_{B} respectively. These values are close to the theoretical free ion values (gJ) for terbium and dysprosium while that of neodymium is smaller than that expected for the free Nd^{3+} ion (*i.e.* $gJ=3.2 \mu_{\text{B}}$). No localized magnetic moment on the iron atoms

is detected, within the accuracy of the neutron powder diffraction experiment. Tables 3–5 give the calculated and observed intensities, together with the adjustable parameters ($z_{\text{R, Si}}, f_{\text{cor}}, \mu_{\text{R}}$) and the lattice parameters. The refined values of the March coefficient are, within the standard errors, the same in the paramagnetic and ordered states, indicating that the correction of the texture effects is realistic. The f_{cor} value is rather large for the neodymium and terbium compounds, whereas the low value reported for DyFeSi is probably due to the special sample holder used in this case.

The temperature dependence of the magnetic intensities recorded step by step between room temper-

TABLE 5. DyFeSi: observed and calculated intensities and refined parameters

hkl	120 K		2 K	
	I_o	I_c	I_o	I_c
001	1.5(2)	1.7	1.6(3)	1.0
101 } 002 } 110 }	108.8(2)	107.0	355.9(2)	368.3
111 } 102 } 003 }	60.1(2)	58.3	295.9(3)	280.5
112 }	418.1(3)	417.9	313.4(4)	308.9
103 }	87.6(4)	88.3	325.0(4)	320.9
200 }	406.4(4)	407.3	92.6(2)	102.6
201 }	385.9(6)	394.0	451.9(3)	443.6
	16.1(4)	8.2	—	—
	$R=0.016$	$r=1.06(2)$	$R=0.026$	$r=1.03(2)$
	$z_{Si}=0.200(5)$	$z_{Dy}=0.676(1)$	$z_{Si}=0.212(10)$	$z_{Dy}=0.670(2)$
				$\mu_{Dy}=9.81(16) \mu_B$
	$a=3.950(2) \text{ \AA}$	$c=6.842(3) \text{ \AA}$	$a=3.924(2) \text{ \AA}$	$c=6.927(3) \text{ \AA}$

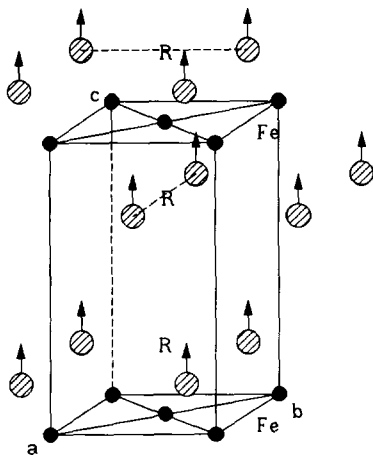


Fig. 4. Magnetic structure of RFeSi (R≡Nd, Tb, Dy) compounds at 2 K.

ature and 2 K gives an R sublattice ordering temperature $T_C = 25(1)$, $125(1)$ and $110(1)$ K for neodymium, terbium and dysprosium respectively, in fair agreement with the bulk magnetization measurements (Table 2). In all three compounds, the magnetic moments obey the normal Brillouin-type temperature dependence (Fig. 5).

For the three compounds, the thermal variation in the lattice parameters (Fig. 6) clearly shows that a strong magnetostriction effect occurs at the Curie point. There is a sensitive c parameter increase and a slight decrease in the basal parameters, whereas the volume anomaly is nearly negligible. Moreover, the importance of the magnetostriction seems to be correlated with the value of the rare earth magnetic moment: weak for NdFeSi in comparison with TbFeSi and DyFeSi (Fig. 6).

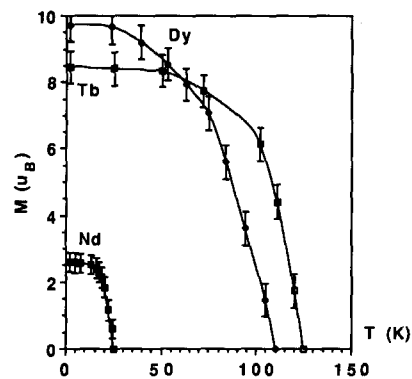


Fig. 5. Temperature dependence of neodymium, terbium and dysprosium magnetic moments in RFeSi compounds.

4. Discussion

The neutron diffraction study confirms the principal results deduced from magnetization measurements, *i.e.* ferromagnetic ordering of the rare earth sublattice at low temperature for neodymium, terbium and dysprosium, but no order in PrFeSi above 2 K, contrary to the PrFe₂Si₂ and PrFeSi₂ compounds.

As in the corresponding RFeSi₂ and RFe₂Si₂ compounds, iron is non-magnetic, whereas the rare earth coupling is ferromagnetic within its (001) plane and the easy magnetization axis is along the stacking direction (c axis) in agreement with the strong anisotropic character of the three series of compounds. The structural relationship is thus confirmed. The observation that all the ferromagnetic compounds have an easy axis magnetization can be related to the occurrence of the strong coercive fields measured in the RFeSi compounds.

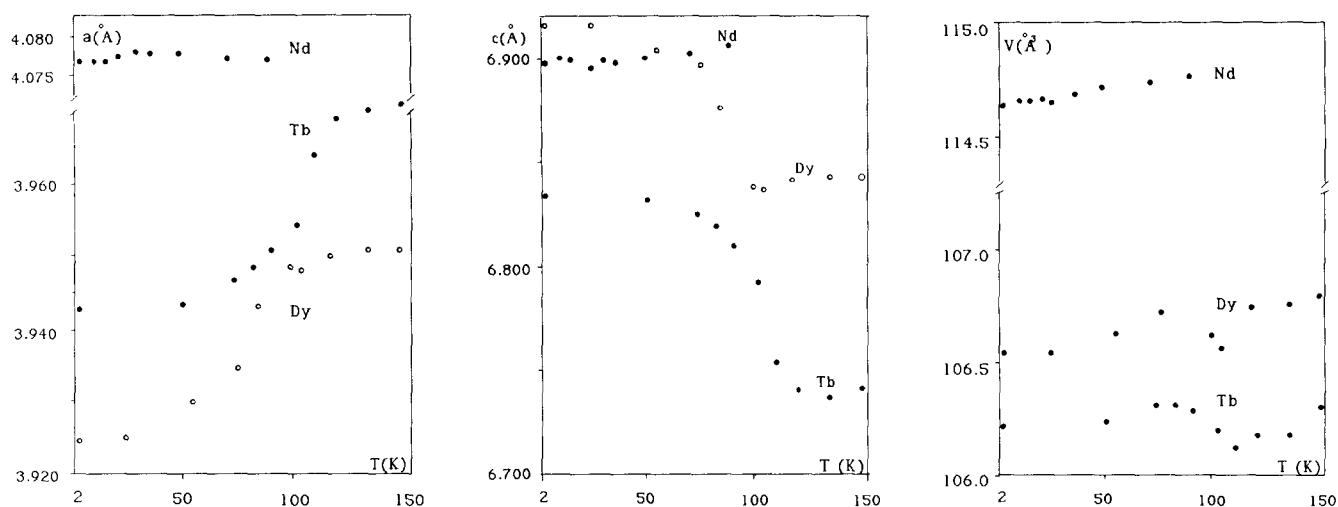


Fig. 6. Thermal variation of the lattice parameters in RFeSi (R≡Nd, Tb, Dy) compounds.

The preferred moment direction θ between μ_R and the c axis is determined by the lowest order term of the anisotropy energy: $E_A = K_1 \sin^2\theta$ ($K_1 > 0$ then μ_R parallel to c) where K_1 is given in standard crystal field theory by [18]

$$K_1 = -\frac{3}{2} \alpha_f \langle r^2 \rangle (1 - \sigma) (2J^2 - J) A_2^0$$

which depends simultaneously on α_f and A_2^0 . Since the Stevens factor α_f depends only on the nature of R, the crucial factor is A_2^0 which is determined by the electrostatic potential due to the environment. For neodymium, terbium and dysprosium, α_f is negative. Assuming that the sign of A_2^0 remains constant for a given site (*i.e.* $A_2^0 > 0$ in this case) this explains the same anisotropic behaviour of the three compounds. In these conditions and assuming that the coercive properties are related to the uniaxial anisotropy, it is surprising to find a rather large coercive field for the samarium compound (Table 2) since samarium has a positive Stevens coefficient α_f .

The transition temperatures are higher than in the other two series. Moreover, the long-range magnetic ordering is ferromagnetic, whereas it is antiferromagnetic in the other series, except for PrFeSi₂ (Table 6).

These differences may be explained if we consider that, in all of these compounds, the prevailing magnetic interactions are of the Ruderman–Kittel–Kasuya–Yosida (RKKY) type and thus depend on the number of conduction electrons and on the R–R distances (Table 7).

In Section 1, we emphasized that there is a relationship between the ThCr₂Si₂, TbFeSi₂ and CeFeSi-type structures: CeFeSi can be described as isolated ThCr₂Si₂-type blocks (including iron atoms); these blocks are connected by Si–Si slabs in TbFeSi₂ (Fig. 7).

TABLE 6. Magnetic ordering and transition temperatures in the RFe₂Si₂, RFeSi₂ and RFeSi compounds

Compound	Coupling	μ_R (μ_B)	$T_{C,N}$ (K)	Reference
PrFe ₂ Si ₂	AF	1.5	8	11
NdFe ₂ Si ₂	AF	3.1	14	12
GdFe ₂ Si ₂	AF	7	8	1
TbFe ₂ Si ₂	AF	8	6	1
DyFe ₂ Si ₂	AF	10	3.8	1
PrFeSi ₂	F	2.57	26	4
NdFeSi ₂	AF	2.50	7	4
PrFeSi	Para	—	—	This work
NdFeSi	F	2.58	25	This work
SmFeSi	F	—	40	This work
GdFeSi	F	(7)	135	This work
TbFeSi	F	8.82	125	This work
DyFeSi	F	9.81	110	This work

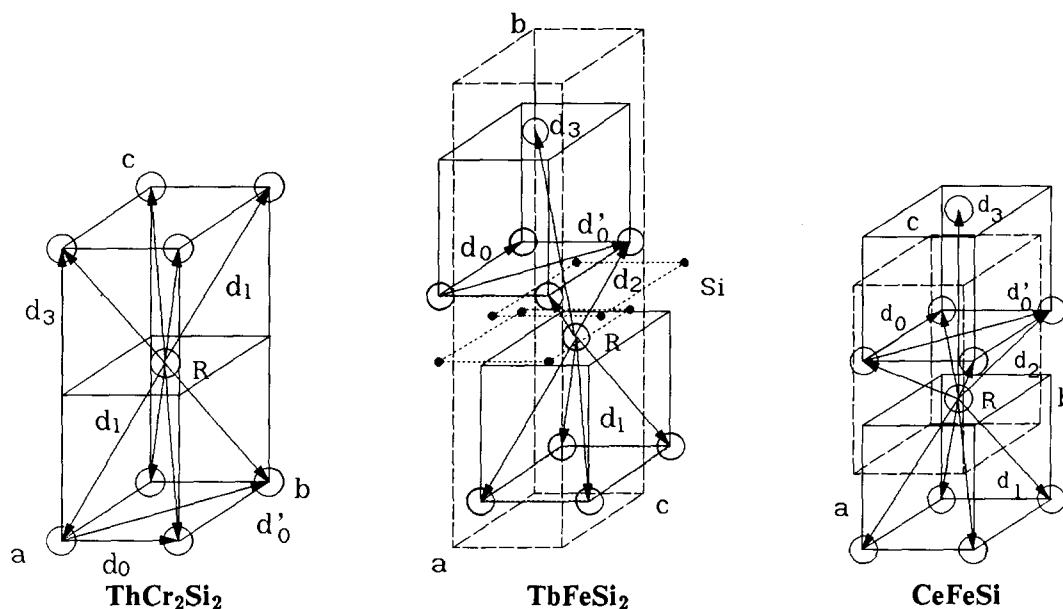
AF, antiferromagnetic; Para, paramagnetic; F, ferromagnetic.

A comparison between the RFe₂Si₂ and RFeSi₂ compounds has been made in a previous paper [4]. Several R–R magnetic couplings must be considered (Table 7, Fig. 7): J_0 within the R planes (d_0 and d'_0); J_1 between R planes making up the ThCr₂Si₂ block (d_1); J_2 and J_3 between nearest (d_2 , in RFeSi₂ compounds only) and next-nearest (d_3) neighbours of adjacent ThCr₂Si₂ blocks respectively.

An analysis of all the iron compounds studied thus far shows that J_0 and J_2 are always positive. For J_1 the situation is more complex. It is probably positive in the ferromagnetic PrFeSi₂ compound. NdFeSi₂ is antiferromagnetic with a sine-modulated magnetic structure. Such an incommensurate structure involves ThCr₂Si₂ blocks in which the moments are ferromagnetically coupled and others in which they are antiferromagnetically coupled [4]. The ⁵⁷Fe Mössbauer study of this compound has shown that 58% of the iron atoms experience a transferred hyperfine field (*i.e.* 58% of

TABLE 7. Main interlayer (R-R) interatomic distances in ThCr_2Si_2 , TbFeSi_2 and CeFeSi -type structures (cf. Fig. 7) (the distances have been calculated for the corresponding neodymium compounds)

Structural type	Local symmetry	Intralayer distance (\AA)		Interlayer distance (\AA)		
		$(4 \times) d_0$	$(4 \times) d'_0$	$(4 \times) d_1$ (ThCr_2Si_2 block)	d_2	d_3
ThCr_2Si_2	$4/mmm$	3.98	5.63	5.75	—	$(2 \times) 10$
TbFeSi_2	mm	4/4.08	5.71	5.69	$(2 \times) 4.03$	$(4 \times) 8.73$
CeFeSi	$4mm$	4.07	5.75	5.32	$(4 \times) 3.77$	$(2 \times) 6.90$

Fig. 7. R-R interatomic distances in CeFeSi -, TbFeSi_2 - and ThCr_2Si_2 -type structures (cf. Table 7).

iron is in a ferromagnetic $\text{Nd-Si-Fe}_2\text{-Si-Nd}$ sheet) and 42% do not. Indeed, the non-commensurate order observed in this compound probably results from the competition between opposite J_1 and J_3 interactions (with probably J_1 positive and J_3 negative [4]).

The RT_2X_2 compounds exhibit a large variety of ordering schemes: collinear ferromagnetism (manganese), four types of collinear antiferromagnetism (iron, cobalt, rhodium, iridium, copper, gold) and also different non-collinear structures (ruthenium, nickel, palladium, iron, silver, osmium) have been discovered [1]. This clearly shows that the magnetic configurations depend not only on the R ion but also on the transition metal element. In the case of RFe_2Si_2 compounds, the magnetic ordering is either the so-called AFII type with half of the $\text{R-Si-Fe}_2\text{-Si-R}$ blocks ferromagnetically coupled (praseodymium, neodymium) or complex sine-modulated magnetic structures (dysprosium, terbium, holmium) where ferromagnetically coupled $\text{R-Si-Fe}_2\text{-Si-R}$ slabs mainly occur. Thus it appears that J_1 seems to be essentially positive (and J_3 negative) for the ternary iron silicides.

In the RFeSi structure J_0 is always positive, and the common in-plane interactions in the three series are

therefore similar. The J_2 exchange (between ThCr_2Si_2 blocks: d_2 , Fig. 7), which acts between R atoms that are separated by rather short interatomic distances (close to those observed in the elemental metallic state, "R-R" direct interaction), is also always positive. Therefore the assumption that J_1 is also positive (as in the other two series) is in agreement with the ferromagnetic behaviour of the RFeSi compounds. Under these conditions J_3 could be positive or frustrated. However, in order to verify these hypotheses, it will be necessary to check the magnetic behaviour of the isotopic RCoSi series since, in the corresponding RCO_2Si_2 compounds, the interlayer R-R coupling in the $\text{R-Si-Co}_2\text{-Si-R}$ blocks is always antiferromagnetic [1]. Such investigations are in progress.

The distances d_1 and d_3 are somewhat smaller and more numerous (Table 7) in the RFeSi series. These results can be correlated with the higher transition temperatures observed in the RFeSi series. On the other hand, it is very surprising that no order occurs in PrFeSi . The values of the magnetic moments measured at 2 K are similar to those observed in the corresponding RFe_2Si_2 compounds: close to the the-

oretical values for the heavy rare earths, but slightly reduced for the neodymium compounds. However, it is worth noting that a large reduction of the praseodymium moment is observed in PrFe₂Si₂ (1.45 vs. 3.20 μ_B) [11], with an order temperature of 6 K compared with 16 K for NdFe₂Si₂. This result can be explained within the framework of the crystal field model which shows that the magnetic moment value depends critically on the higher order crystal field parameters, particularly on B₄⁴ [11]. A more important reduction of the moment in PrFeSi (connected with its particular environment, Fig. 1) may perhaps explain the lack of ordering of the praseodymium sublattice above 2 K in this compound. The possibility that, owing to the crystal field splitting, the lowest level may be a non-magnetic singlet level may also explain the lack of ordering of the praseodymium sublattice.

5. Conclusions

The determination of the magnetic properties of RFeSi compounds provides new information on the magnetic interactions in rare earth ternary iron silicides and enables comparisons to be made with the closely related RFeSi₂ and RFe₂Si₂ compounds.

The RFeSi (R≡Nd–Sm, Gd–Dy) compounds exhibit ferromagnetic ordering of the R sublattices at low temperatures, whereas no magnetic order occurs in PrFeSi above 2 K. In addition, some of these compounds exhibit very high coercive fields (TbFeSi: approximately 9 kG at 4.2 K) attesting to a strong uniaxial anisotropy as also observed in RFeSi₂ and RFe₂Si₂ compounds. No local moment on the iron sublattice was detected in any of the investigated compounds. Although neutron diffraction is not sensitive to very small magnetic moments, the absence of a local iron moment is supported by the behaviour of the isostructural LaFeSi and CeFeSi compounds which were shown to be Pauli paramagnets.

The study of the magnetic ordering of RFeSi (neodymium, terbium, dysprosium) provides useful information on the rare earth anisotropy and exchange interactions. The stability of the collinear magnetic structures consisting of ferromagnetic (001) planes (with moments perpendicular to the planes) may be ascribed either to anisotropic exchange interactions arising from orbital polarization of the conduction electrons or to single ion anisotropy plus exchange interactions. The orientation of the R moments with respect to the crystal [001] axis is probably determined by the sign of A₂⁰. In the case of the RFeSi (R≡Nd, Tb, Dy) compounds, an [001] easy axis direction indicates that A₂⁰ should be positive. The influence of crystal field effects may also explain the partial quenching of the neodymium

moment, which is somewhat smaller than the free ion value, and the absence of magnetic ordering in PrFeSi.

The magnetic structures are very similar to those found in most of the corresponding ThCr₂Si₂- and TbFeSi₂-type compounds in agreement with the underlying structural relationships. In all of these compounds, the long-range magnetic ordering along the stacking axis depends on interactions of the RKKY type.

Finally, ⁵⁷Fe Mössbauer spectroscopy will provide additional information on the magnetic behaviour of these phases. A comparison of the transferred hyperfine field on the iron atoms will enable us to check the simple RKKY systematics and the R moment direction in GdFeSi and SmFeSi. Moreover, ¹⁵⁵Gd and ¹⁶¹Dy Mössbauer spectroscopy, through the determination of the electric field gradient, may also provide information on the sign of A₂⁰. These experiments are in progress.

Acknowledgments

We are indebted to the Institut Laue Langevin (Grenoble) for the provision of research facilities. Magnetic measurements were undertaken at the Service Commun de Magnetométrie de l'Université de Nancy I. We are grateful to Dr J. Hubsch (responsible for the magnetometer) and Dr J. L. Soubeyroux (responsible for the D1b spectrometer) for their help during the measurements.

References

- 1 A. Szytula and J. Leciejewicz, Magnetic properties of ternary intermetallic compounds of the RT₂X₂ type, in K. A. Gschneidner, Jr. and L. Eyring (eds.), *Handbook on the Physics and Chemistry of Rare Earths*, Vol. 12, 1989, Chapter 83, Elsevier, p. 133.
- 2 G. Venturini, B. Malaman, M. Meot-Meyer, D. Fruchart, G. Le Caer, D. Malterre and B. Roques, *Rev. Chim. Minér.*, **23** (1986) 162.
- 3 B. Malaman, G. Venturini, L. Pontonnier and D. Fruchart, *J. Magn. Magn. Mater.*, **86** (1990) 349.
- 4 B. Malaman, G. Venturini, L. Pontonnier, D. Fruchart, G. Le Caer, K. Tomala and J. P. Sanchez, *Phys. Rev.*, **41** (7) (1990) 4700.
- 5 V. I. Yarovets and Yu. K. Gorelenko, *Vestn. L'vovsk. Univ., Ser. Khim.*, **23** (1981) 20.
- 6 O. I. Bodak, E. I. Gladyshevskii and P. I. Kripyakevich, *Zh. Struct. Khim.*, **11** (1970) 283.
- 7 L. D. Knigenko, I. R. Mokra and O. I. Badok, *Vest. L'vovsk. Univ., Ser. Khim.*, **19** (1977) 68.
- 8 O. I. Bodak, E. I. Gladyshevskii, E. M. Levin and R. V. Lutsiv, *Dopov. Akad. Nauk. Ukr. RSR, Ser. A*, **12** (1977) 1129.
- 9 Yu. V. Stadnik, Yu. K. Gorelenko, R. V. Skolozdra, V. I. Yarovets and O. I. Bodak, *Splavy Redk. Tugoplauk Met. Osob Fiz. Svoistvami M*, (1979) 124.
- 10 E. M. Levin, O. I. Bodak, Yu. V. Zhipa and N. N. Vashchishchuk, *Dopov. Akad. Nauk. Ukr. RSR, Ser. A*, **6** (1983) 78.
- 11 B. Malaman, G. Venturini, A. Blaise, J. P. Sanchez, G. Amoretti, *Phys. Rev. B*, (1992) in the press.

- 12 H. Pinto and H. Shaked, *Phys. Rev. B*, 7 (1973) 3261.
- 13 W. A. Dollase, *J. Appl. Crystallogr.*, 19 (1986) 267.
- 14 A. March, *Z. Kristallogr.*, 81 (1932) 285.
- 15 A. J. Freeman and J. P. Declaux, *J. Magn. Magn. Mater.*, 69 (1979) 61.
- 16 C. Stassis, H. W. Deckman, B. N. Harmon, J. P. Declaux and A. J. Freeman, *Phys. Rev. B*, 15 (1977) 369.
- 17 P. Wolfers, *J. Appl. Crystallogr.*, 23 (1990) 554.
- 18 W. E. Wallace, *Rare Earth Intermetallics*, Academic Press, New York, 1973, Chapter 3.